Journal of the Serbian Chemical Society
JSCS-info@shd.org.rs • www.shd.org.rs/JSCS
J. Serb. Chem. Soc. *86* (6) 615–624 (2021)
JSCS–5448
Original scientific paper

CO oxidation over alumina monolith impregnated with oxides of copper and manganese

THIEN HUU PHAM[1]*, VIET BANG BUI[1] and HA AN QUOC THAN[1,2]

[1]*Institute of Applied Materials Science, Vietnam Academy of Science and Technology, No 1A TL 29, Thanh Loc Ward, District 12, Ho Chi Minh 700000, Vietnam;* [2]*Graduate University of Science and Technology, Vietnam Academy of Science and Technology, 18 Hoang Quoc Viet, Cau Giay, Ha Noi 10072, Vietnam*

(Received 9 May 2020, revised 10 January, accepted 15 January 2021)

Abstract: In this work, simple methods for the preparation of highly efficient heterogeneous nanocatalysts for the low-temperature oxidation of CO are described. The main advantages of the reaction are high yields. The catalysts based on oxides of copper and manganese supported on alumina monoliths were prepared by different methods: plasma corona discharge and wet impregnation. Structure and physical properties of catalysts were characterized by FT-IR, XRD, TEM, EDX and TG/DTA. The results showed that the use of a plasma corona discharge at atmospheric pressure for the preparation of the catalysts resulted in smaller particle size and uniform dispersion when compared with the catalysts prepared by wet impregnation methods. The catalytic activities of these catalysts were investigated for complete oxidation of carbon monoxide (3000 ppm) to carbon dioxide in the air at atmospheric pressure. On a single oxide catalyst, 10CuO/monolith was better than 10MnO_2/monolith under the same experimental conditions. With multi-oxide catalysts, all catalyst samples are more active than a single-oxide catalyst with the same impregnated content. In particular, the catalyst prepared by plasma corona discharge indicates the best oxidation capacity of carbon monoxide.

Keywords: oxidation of carbon monoxide; single-oxide catalysts; multi-oxide catalysts; corona discharge; alumina monolith; wet-impregnation.

INTRODUCTION

Carbon monoxide (CO) is a common contaminant of indoor and outdoor environments. Along with volatile organic compounds (VOCs) and nitrogen oxides (NO_x), CO is one of the main causes of air pollution and affects human health.[1,2] Therefore, it is especially important to find a solution to CO removal from the air. At present, an effective solution for CO removal is to use a catalytic oxidation technique. In this method, the catalyst plays a key role in the treatment

* Corresponding author. E-mail: thieniams@gmail.com
https://doi.org/10.2298/JSC200509004P

efficiency as well as a change in the temperature of the oxidation reaction. Catalysts based on noble metals (Pd, Pt, Rh) exhibit a high activity for CO oxidation.[3–5] However, the steady increase of noble metal prices, their tendency to sinter and deactivation by carbon formation pushes the development of alternative catalytic technologies and catalytic materials. Recently, studies have turned to catalysts based on transition metals (Cu, Mn, Co, Fe,...). Many studies have shown that catalysts based on Cu, Co and Mn are very efficient for CO oxidation at low temperatures.[6]

A multi-oxide catalyst on a transition metal base has recently been studied and found to be effective for the treatment of VOC and CO emissions.[7] In these studies, oxidation is affected by the interaction between the active phases of transition metals due to the formation of strange phases during the preparation process. Morales[8] studied the effect of the copper content in manganese on complete oxidation of ethanol and propane, showing that the addition of a small amount of copper helped prevent manganese oxide from entering the crystal structure, increases the formation of voids and the presence of $Cu_{1.5}Mn_{1.5}O_4$ phase and increases their reduction ability, thus achieving better catalytic performance in ethanol combustion.

Many factors influence the properties of the catalyst, of which one of the most important is the catalyst preparation method. With this in mind, various methods, such as wet-impregnation (WI),[9] deposition-precipitation (DP)[10] and atmospheric plasma discharge, have been investigated.[11–13] Recently, one of the current catalytic preparation methods of interest has been corona plasma discharge at atmospheric pressure. Many reports show that the use of a plasma helps affect a significant rise in catalytic activity and a small particle size-dispersion is achieved compared to the other conventional methods.

This work was aimed at examining the influence of different preparation methods on the catalyst performance based on alumina monoliths impregnated with oxides of copper and manganese. Furthermore, the catalytic activities of these catalysts were investigated for complete oxidation of carbon monoxide in the air at atmospheric pressure.

EXPERIMENTAL

Chemicals

$Cu(NO_3)_2{\cdot}3H_2O$ (>99.5 %, Sigma Aldrich), Mn $(NO_3)_2$ (99 %, Sigma Aldrich), and alumina monoliths with a cell density of 62 cells cm^{-2} – Nanxiang-Jiangxi, China. All the chemicals were used without further purification.

Catalysts preparation

The catalysts with 10 wt. % metal loading (5 wt. % Cu and 5 wt. % Mn) were prepared by different methods: wet-impregnation (WI) and non-thermal plasma (NTP).

WI method. The alumina monoliths was the first impregnated with a solution of $Cu(NO_3)_2$ $3H_2O$ and/or Mn $(NO_3)_2$. After evaporating under vacuum at 353 K, the sample

was dried at 383 K for 12 h and heated at 773 K for 5 h in air with a heating rate of 276 K min^{-1}. These samples were denoted as 10CuO/Monolith, 10MnO_2/Monolith and 5CuO––5MnO_2/Monolith, respectively.

NTP method. The non-thermal plasma technique used for this preparation was corona discharge as Fig. 1. This process is similar to the WI method. However, after evaporating under vacuum at 353 K, the sample was dried at 383 K for 12 h. The precursor was placed in the corona plasma discharge region using a cylindrical quartz tube located and centered on the holder base plate, which consisted of a continuous flow air supplying the system. The corona plasma discharge reactor was powered by a homemade high voltage direct current generator: 18 kV and 1.5 kHz. The sample was denoted as 5CuO–5MnO_2/Monolith (Plasma).

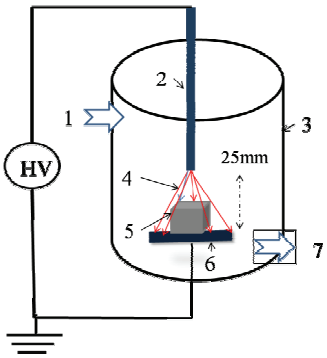

Fig. 1. The schematic diagram of the corona plasma discharge system; 1 – feed-gas system; 2 – needle electrodes; 3 – quartz tube; 4 – corona plasma discharge region; 5 – catalyst samples; 6 – plate electrode; 7 – air outlet (gas-outlet).

Catalyst characterization

Physicochemical characterization of the prepared catalyst was performed by different modern techniques such as Fourier transform infrared (FT-IR), X-ray diffraction (XRD), transmission electron microscopy (TEM), energy-dispersive X-ray (EDX) and thermogravimetric and differential thermal analysis (TG/DTA). In particular, the FT-IR spectra were measured at spectral resolution 4 cm^{-1} between 4000–400 cm^{-1} range using a Perkin Elmer Frontier 1600 series spectroscope. XRD patterns of the catalyst materials were recorded with D8 Advance-Bruker D5005 diffractometer using monochromatic high-intensity CuKα radiation (λ = 0.15418 nm) at the scanning rate of 0.03° s^{-1} in the scanning range from 20 to 80°. TEM images were taken with a JEOL JEM-1010 (Japan) at an acceleration voltage of 200 kV. The EDX analysis with 20 kV accelerated voltage was realized with EDX-8000. Finally, the simultaneous thermal analysis (TG/DTA) of the after dried samples was performed in a Q500 TA-Instruments apparatus under atmospheric pressure at a heating rate of 283 K min^{-1}, from 303 to 1073 K under a dynamic (50 mL/min) nitrogen atmosphere.

Catalytic performance

Catalytic properties of the studied samples for CO total oxidation in air were tested under the following conditions: The total flow was 450 mL min^{-1} at a volume rate (GVSH) of 5000 h^{-1}. The initial concentration of CO was fixed at 3000 ppm. The CO concentration in the reaction was analyzed *in situ* by Testo 320 LX (0563 6032 72 (Germany) and then re-analyzed by GC Clarus device (USA), a column packed with ZV-95, length 3 m, diameter 5.8 mm.

RESULTS AND DISCUSSION

X-Ray diffraction diagram (XRD)

The X-ray diffraction (XRD) patterns of the catalysts are shown in Fig. 2.

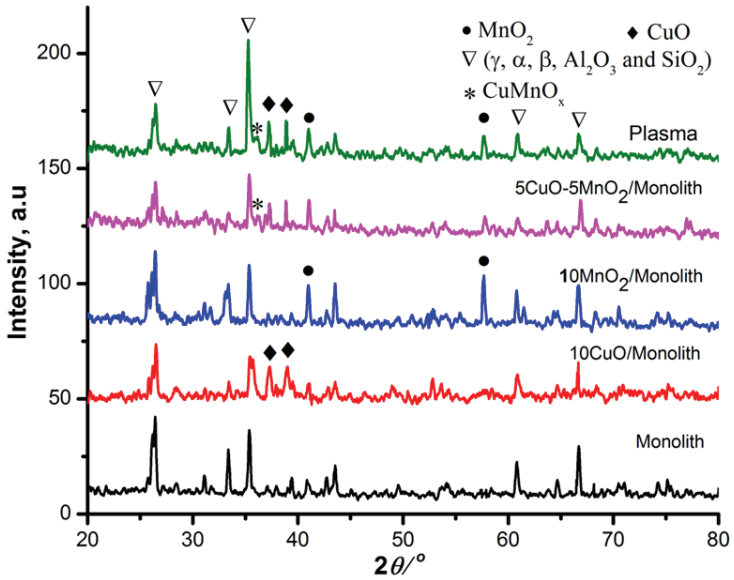

Fig. 2. The X-ray diffraction (XRD) patterns of the catalysts.

As indicated in Fig. 2, the main components of the alumina monolith substrate were α-Al_2O_3, β-Al_2O_3, γ-Al_2O_3 and SiO_2 with specific diffraction signals at 2θ 25.9, 33.6 and 36.1°. On the single-oxide catalysts, the copper-based catalysts have typical diffraction signals of the CuO phase (2θ 35.7 and 38.8°, JCPDS 80-1268). On the manganese-based catalyst, the characteristic diffraction signals are those of the MnO_2 phase (2θ 41.1, 44.7 and 57.7°, JCPDS 44-0141). On multi-oxide catalysts, besides the diffraction signals of CuO and MnO_2 phases, on the X-ray diffraction diagram also appear a diffraction signal of weak intensity of the $CuMnO_x$ phase (2θ = 37.2°). These results are similar to those of Dey.[14] Compared with the catalysts prepared by the wet-impregnation method, in the diffraction pattern of 5CuO–5MnO_2/Monolith-corona (Plasma) appeared narrow high intensity peaks of CuO and MnO_2. This difference could be explained by the interaction of the reactive species produced by plasma discharges, such as $O^{\bullet}$, $N^{\bullet}$, $NO^{\bullet}$, $OH^{\bullet}$, O_3 and H_2O_2, with the catalyst sample in the preparation process led to changes in the phase structure properties.

Fourier transform infrared spectrum (FT-IR)

The FT-IR spectra of the samples are shown in Fig. 3.

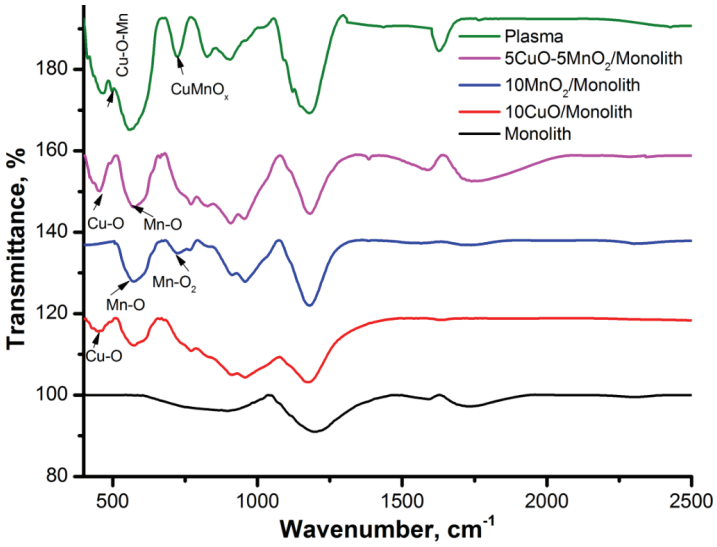

Fig. 3. FT-IR spectra of the catalysts.

According to the results in Fig. 3, the absorption peaks due to Cu–O bonds in the CuO phase structure are found in the region 420 to 500 cm^{-1} for 10CuO/ /Monolith catalyst. This result is similar to the studies by Dubal *et al.*[15] This shows that the CuO phase was successfully impregnated on alumina monolith. In the spectra of the $10MnO_2$/Monolith catalyst, characteristic vibrations of Mn–O bonds are found at 535 and 690 cm^{-1} for the MnO_2 phase. This result is also in agreement with the studies of Aghazadeh.[16] In multi-oxide catalysts case, all catalysts also indicated typical vibrations of CuO and MnO_2 phases impregnated on alumina monolith.

Transmission electron microscopy (TEM)

Typical TEM results for the catalysts are shown in Fig. 4.

According to the TEM images, both catalysts possessed spherical morphology (<50 nm). Fig. 4a and b show the presence of CuO and MnO_2 phases impregnated on the alumina monolith for both single-oxide catalysts with particle sizes ranging from 30–50 nm. In addition, the results also show a fairly even dispersion of these active phases on the supports. On a multi-oxide catalyst (Fig. 4c), the size of the active phase and the dispersion are similar to the single-oxide catalyst. However, with multi-oxide catalysts prepared by plasma discharge technique indicate a different surface morphology. High dispersion and small active particle size (10–20 nm) were found for this catalyst (Fig. 4d). This suggests that the use of plasma discharges during the preparation process drastically changed the catalytic properties leading to increased catalytic oxidation.

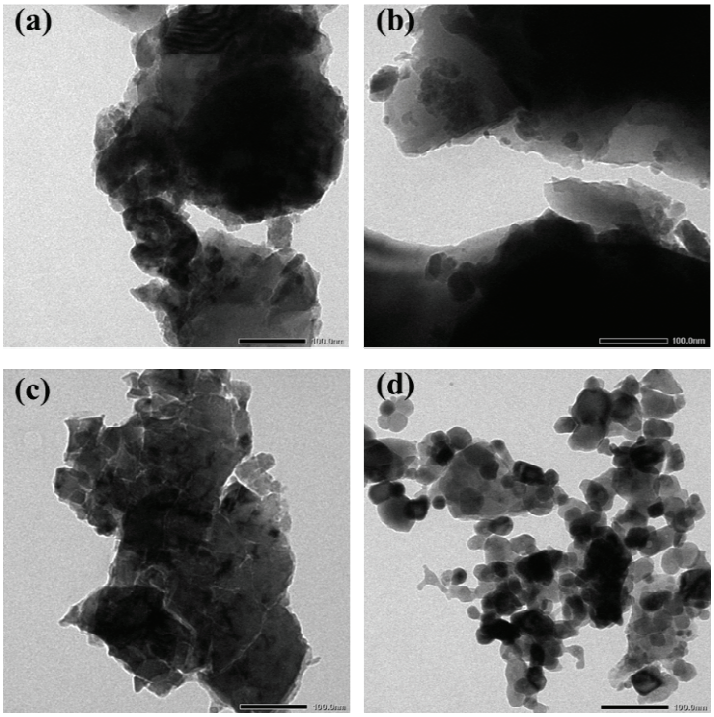

Fig. 4. TEM images of 10CuO/Monolith (a), 10MnO_2/monolith (b), 5CuO–5MnO_2/Monolith (c) and 5CuO–5MnO_2/Monolith (Plasma) (d).

Besides, to test the impregnation of Cu and Mn metals onto monolith, EDX analysis method used to determine metal content in the monolith (Fig. 5 and Table I). The results indicated the presence of elemental Cu and Mn in the 5CuO–5MnO_2/Monolith (Plasma). It could be concluded that the impregnation of the active phase on support by the non-thermal plasma technique was successful.

Thermogravimetric and differential thermal analysis (TG/DTA)

The TG/DTA analysis of the samples showed a major mass loss of about 11 % in the range of 303 to 1073 K, which was due to the elimination of the majority of the nitrate compounds (Fig b). The first mass loss step in the TGA plot occurred between 273–393 K, corresponding to the weak endothermic peak in the DTA curve at 343 K, which was caused by dehydration. In the last mass loss step, a drastic weight loss at 473–573 K resulted from the combustion of nitrate compounds and NO_x formation *via* the decomposition of nitrate compounds as suggested by the exothermic peak around 508 and 528 K in the DTA curve. No further mass loss occurred above 573 K, indicating completion of combustion and the formation of the expected oxide CuO–MnO_2 phase.

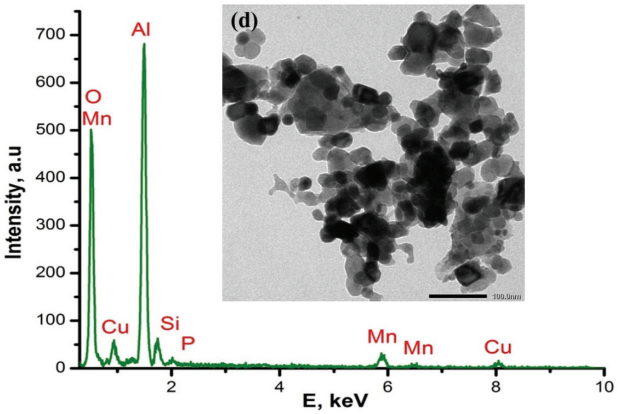

Fig. 5. EDX analysis of the 5CuO–5MnO_2/Monolith (Plasma) catalyst.

TABLE I. Elemental composition analysis of 5CuO–5MnO_2/Monolith (Plasma) catalyst

Element	Amount, wt. %	Amount, at. %
O	48.34	62.28
Al	32.75	26.98
Si	4.98	5.70
P	0.59	0.39
Mn	6.29	2.36
Cu	7.05	2.29
Total	100.00	–

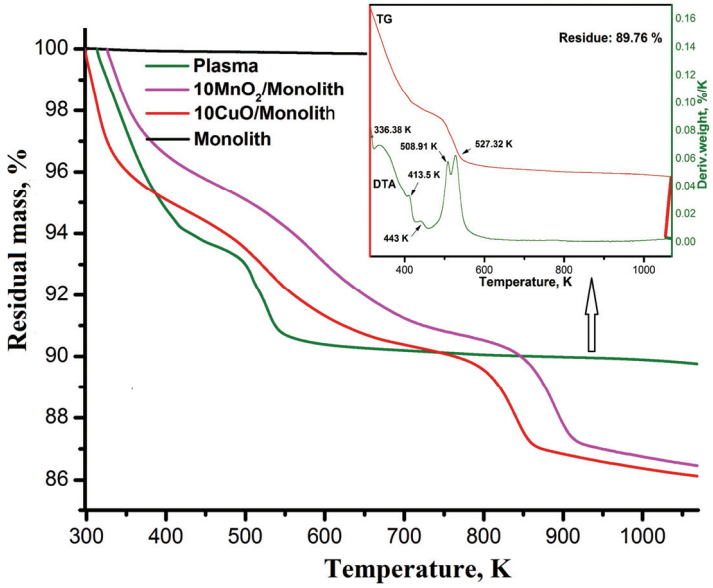

Fig. 6. TG/DTA analysis of the catalysts.

Catalytic activity for complete oxidation of CO

The complete oxidation of CO to CO_2 was performed over various catalysts according to temperature. The conversion of CO according to temperature over the catalysts is shown in Fig. 7.

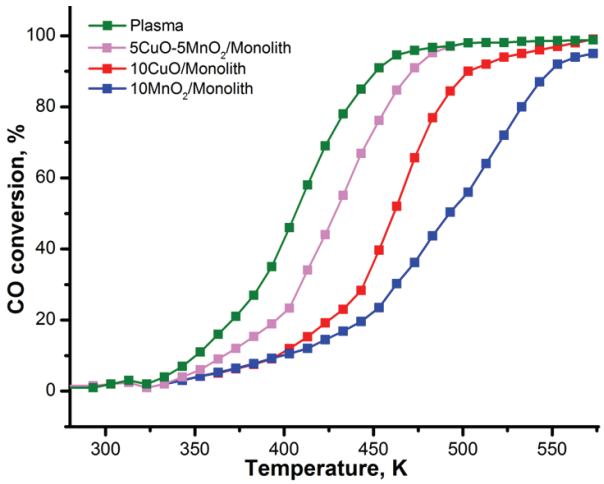

Fig. 7. CO conversion over the different catalysts according to temperature.

The results indicated that complete oxidation of CO (>98 % conversion) was achieved at temperatures above 503 K for both multi-oxide catalysts. Whereas, the conversion was only 90 % for single oxide 10CuO/ /Monolith catalyst and 56 % conversion for $10MnO_2$/Monolith catalyst.

A comparison of the activity of the catalysts in different temperature ranges is also presented in Table II.

TABLE II. Conversion of CO (%) at different temperatures and over different catalysts

Catalyst	Temperature, K		
	373	423	573
10CuO/Monolith	6.3	19.2	99.0
$10MnO_2$/Monolith	6.4	14.5	95.0
5CuO–$5MnO_2$/Monolith	12.1	44.1	98.7
5CuO–$5MnO_2$/Monolith (Plasma)	21.2	69.3	98.8

At 373 K, the difference in CO treatment efficiency of the four catalysts is negligible. As the temperature increased, the catalyst conversion rates began to diverge. At 423 K, the 5CuO–$5MnO_2$/Monolith (Plasma) catalyst yielded 1.6 times higher conversion than the 5CuO–$5MnO_2$/Monolith catalyst, 3.6 times higher than 10CuO/Monolith and 4.8 higher than $10MnO_2$/Monolith. When the reaction temperature reached 573 K, total oxidation of CO was obtained for all

catalysts. These results could be explained by the 5CuO–5MnO_2/Monolith (Plasma) catalyst treated by the plasma discharge caused CuO–MnO_2 particles to disperse highly and evenly on the surface of the alumina monolith as nanoparticles. This would increase the interaction with CO in the reaction. Besides, the increase in activity is also due to the appearance of a new active phase $CuMnO_x$ from the interaction between the oxides of copper and manganese.

The catalytic activity for CO oxidation is shown in the following order: 5CuO–5MnO_2/Monolith (Plasma) catalyst > 5CuO–5MnO_2/Monolith catalyst > 10CuO/Monolith > 10MnO_2/Monolith.

In general, the intervention of plasma discharge during the preparation process changed the catalytic properties leading to high treatment efficiency for CO removal. In summary, the 5CuO–5MnO_2/Monolith (Plasma) catalyst shows an efficient oxidation of CO at lower temperatures than the other studied cases.

CONCLUSIONS

First, single-oxide and multi-oxide catalysts based on copper and manganese-impregnated on alumina monolith were successfully prepared by two different methods. The results indicate that the differences in the preparation methods play an important role in the determination of the physicochemical properties as well as the oxidative activities of the catalysts. Secondly, on a single oxide catalyst, the 10CuO/Monolith sample was better than a 10MnO_2/Monolith sample. With multi-oxide catalysts, all catalyst samples are more active than single-oxide catalysts at the same impregnated content. Finally, the catalyst prepared by the plasma discharge method showed the best oxidation of CO capacity when compared with the catalysts prepared by the wet-impregnation method under the same experimental conditions.

Acknowledgment. This research was funded by the Vietnam National Foundation for Science and Technology Development (NAFOSTED, Grant No. 103.99-2016.67).

ИЗВОД

ОКСИДАЦИЈА УГЉЕН-МОНОКСИДА НА МОНОЛИТИМА ГЛИНИЦЕ ИМПРЕГНИСАНИМ ОКСИДИМА БАКРА И МАНГАНА

THIEN HUU PHAM[1], VIET BANG BUI[1] и HA AN QUOC THAN[1,2]

[1]*Institute of Applied Materials Science, Vietnam Academy of Science and Technology, No 1A TL 29, Thanh Loc Ward, District 12, Ho Chi Minh 700000, Vietnam* и [2]*Graduate University of Science and Technology, Vietnam Academy of Science and Technology, 18 Hoang Quoc Viet, Cau Giay, Ha Noi 10072, Vietnam*

У овом раду описани су припрема и перформансе катализатора, користећи једноставну методу и високо ефикасан хетерогени нанокатализатор. Главна предност реакције су високи приноси оксидације CO на ниској температури. Катализатори на бази оксида бакра и мангана на монолитној глиници као носачу припремљени су различитим методама: корона пражњењем у плазми и мокром импрегнацијом. Структура и физичка својства катализатора окарактерсани су FT-IR, XRD, TEM, EDX и TG/DTA методама. Резултати су показали да коришћење корона пражњења у плазми, при атмосферском притиску, у процесу припреме катализатора даје мању величину честица и равномер-

нију дисперзију у поређењу са катализаторима припремљеним методама влажне импрегнације. Каталитичке активности ових катализатора су испитане за потпуну оксидацију угљен-моноксида (3000 ppm) у угљен-диоксид у ваздуху, при атмосферском притиску. При поређењу појединачних оксидних катализатора, 10CuO/монолит је био ефикаснији од $10MnO_2$/монолита у при истим експерименталним условима. Код мултиоксидних катализатора, сви узорци катализатора су активнији од монооксидног катализатора у истом импрегнираном садржају. Конкретно, катализатор припремљен корона пражњењем у плазми показује најбољи оксидациони капацитет угљен-моноксида (CO).

(Примљено 9. маја 2020, ревидирано 10. јануара, прихваћено 15. јануара 2021)

REFERENCES

1. H. Kinoshita, H. Türkan, S. Vucinic, S. Naqvi, R.Bedair, R. Rezaee, A. Tsatsakis, *Toxicol. Rep.* **7** (2020) 169 (https://doi.org/10.1016/j.toxrep.2020.01.005)
2. R. J. Levy, *Neurotoxicol. Teratol.* **49** (2015) 31 (https://doi.org/10.1016/j.ntt.2015.03.001)
3. J. Xu, T. White, P. Li, C. He, J. Yu, W. Yuan. Y.-F. Han, *J. Am. Chem. Soc.* **132** (2010) 10398 (https://doi.org/10.1021/ja102617r)
4. A. S. Ivanova, E. M. Slavinskaya, R. V. Gulyaev, V. I. Zaikovskii, O. A. Stonkus, I. G. Danilova. L. M. Plyasova, I. A. Polukhin, A. I. Boronin, *Appl. Catal. B: Environ.* **97** (2010) 57 (https://doi.org/10.1016/j.apcatb.2010.03.024)
5. H. Huang, D. Y. C. Leung, D. Ye, *J. Mater. Chem.* **21** (2011) 9647 (https://doi.org/10.1039/C1JM10413F)
6. Y. Lang, J. Zhang, Z. Feng, X. Liu, Y. Zhu, T. Zeng, Y. Zhao, R. Chen, B. Shan, *Catal. Sci. Technol.* **8** (2018) 5490 (https://doi.org/10.1039/C8CY01263F)
7. D. A. Aguilera, A. Perez, R. Molina, S. Moreno, *Appl. Catal., B* **104** (2011) 144 (https://doi.org/10.1016/j.apcatb.2011.02.019)
8. M. R. Morales, B. P. Barbero, L. E. Cadús, *Fuel* **87** (2008) 1177 (https://doi.org/10.1016/j.fuel.2007.07.015)
9. P. W. Park, J. S. Ledford, *Appl. Catal., B* **15** (1998) 221 (https://doi.org/10.1016/S0926-3373(98)80008-8)
10. K. Y. Koo, U. H. Jung, W. L. Yoon, *Int. J. Hydrogen Energy* **39** (2014) 5696 (https://doi.org/10.1016/j.ijhydene.2014.01.128)
11. Z.-H. Li, S.-H. Tian, H.-T. Wan, H.-B. Tian, *J. Mol. Catal., A* **211** (2004) 149 (https://doi.org/10.1016/j.molcata.2003.10.003)
12. W. Hua, L. Jin, X. He, J. Liu, H. Hu, *Catal. Commun.* **11** (2010) 968 (https://doi.org/10.1016/j.catcom.2010.04.007)
13. M. H. Chen, W. Chu, X. Y. Dai, X. W. Zhang, *Catal. Today* **89** (2004) 201 (https://doi.org/10.1016/j.cattod.2003.11.027)
14. S. Dey, G. C. Dhal, D. Mohan, R. Prasad, *Bull. Chem. React. Eng. Catal.* **12** (2017) 437 (https://doi.org/10.9767/bcrec.12.3.900.437-451)
15. D. P. Dubal, G. S. Gund, C. D. Lokhande, R. Holze, *Mat. Res. Bull.* **48** (2013) 923 (https://doi.org/10.1016/j.materresbull.2012.11.081)
16. M. Aghazadeh, M. Asadi, M. G. Maragheh, M. R. Ganjali, P. Norouzi, F. Faridbod, *App. Surf. Sci.* **364** (2016) 726 (https://doi.org/10.1016/j.apsusc.2015.12.227).